
CHEMICAL KINETICS AND CATALYSIS

The Kinetics of Low-Temperature Oxidation of Cobalt Nanoparticles in Porous Media

A. V. Mugtasimov^a, N. V. Peskov^b, G. V. Pankina^a, P. A. Chernavskii^a, and V. V. Lunin^a

^a Faculty of Chemistry, Moscow State University, Moscow, Russia

^b Faculty of Computational Mathematics and Cybernetics, Moscow State University, Moscow, Russia

e-mail: chern@kge.msu.ru

Received February 25, 2010

Abstract—The kinetics of oxidation of Co nanoparticles used in heterogeneous catalysis in silica gels and alumina with various porous structures was studied at room temperature. A mathematical model describing processes in the system was suggested. The experimental observations were qualitatively explained.

Keywords: kinetics, low-temperature oxidation, cobalt nanoparticles, porous media.

DOI: 10.1134/S0036024411020257

INTRODUCTION

Studies of the kinetics and mechanism of low-temperature oxidation of metal nanoparticles acquire practical importance in view of rapidly developing nanotechnologies. Low-temperature oxidation (temperature range from ~280 to ~400 K) is substantially different from high-temperature processes, which are well described by the Wagner theory [1], in which a key role is played by diffusion.

The theory of low-temperature oxidation or oxidation in thin films was for the first time formulated by Cabrera and Mott (C–M theory) [2]. It involves the appearance of an electric potential (Mott potential) between oxide–adsorbed oxygen and oxide–metal boundaries at the initial time moment. The corresponding electric field can pull out metal atoms and move them toward the outside oxide surface, where an oxide film grows. The theory qualitatively correctly describes the formation of planar thin oxide films, but ignores potential gradients in films and assumes that the diffusion coefficients of metal ions, oxygen ions, electrons, and vacancies are constant. The picture is considerably complicated in spherical particles compared with planar films, where the presence of size effects is obvious. In part, these effects are caused by the dependence of the Mott potential on the radius of particles. Considering this circumstance, it can be shown [3] that the rate of oxidation increases as the radius of particles decreases.

The experimental data obtained comparatively recently make us take a different view of the oxidation of nanoparticles of certain metals and introduce additional limitations into the C–M theory. For spherical particles, the Kirkendall effect [4] is of special importance. This effect is a consequence of the difference of

diffusion coefficients in a binary system and, with metal oxidation, manifests itself as the difference of the diffusion coefficients of oxygen and metal ions. Because of the difference of the diffusion coefficients of metal and oxygen ions (for Co, $D_{\text{oxygen}} < D_{\text{metal}}$), the accumulation and subsequent condensation of vacancies occurs at the metal–oxide boundary, which results in the formation of cavities [5, 6, 7]. Characteristically, the condensation of vacancies causes the formation of “bridges” at the initial oxidation stage. These bridges connect the oxide shell with the metallic nucleus, and the diffusion of metal ions and electron tunneling occur through them [8].

The formation of cavities at the metal–oxide boundary should likely cause a more substantial decrease in the rate of oxidation than is predicted by the C–M theory, because, as vacancies are accumulated and condensed, the real metal–oxide separation surface through which metal ions diffuse decreases. Earlier, in works concerned with the formation of spherical cavities in the oxidation of metal nanoparticles, most attention was given to systems in which nanoparticles were dispersed in a liquid inert medium [5] or were obtained by ionic sputtering in a high vacuum and subsequently deposited on a carbon substrate [6]. Studies were performed by high-resolution transmission electron microscopy. As concerns the kinetics of oxidation of metal nanoparticles, the corresponding information is exceedingly scarce.

The kinetics and mechanism of oxidation of metal nanoparticles in pores of an inert carrier, as, for instance, in heterogeneous metal deposited catalysts, are often of interest for applications. In such systems, in addition to the oxidation of nanoparticles, oxygen mass transfer in carrier pores can occur. In this work,

Properties of Co/porous carrier samples

s , m ² /g	\bar{d} , nm	Sample	x_{Co} , %	\bar{D} , nm	σ^2	S_{sp} , m ² /g
Co/SiO ₂						
380	6	5%Co/Q-6	6	6	5	6.7
		20%Co/Q-6	14.5	10	8	9.7
320	10	5%Co/Q-10	5.2	6.9	3	4.9
		20%Co/Q-10	11	15	26	4.9
180	15	5%Co/Q-15	3.9	7.5	3	3.7
		20%Co/Q-15	14	13	15	7.2
100	30	5%Co/Q-30	4.9	8	5	4.1
		20%Co/Q-30	15	11	9	9.1
Co/Al ₂ O ₃						
380	8	5%Co/E-380	2	7	3	2
		20%Co/E-380	13	7	4	12
200	10	5%Co/E-200	3	8	4	2.5
		20%Co/E-200	13.6	7	9	13
90	20	5%Co/E-90	4.2	6	4	4.7
		20%Co/E-90	11.3	8	9	9.4

Note: s is the specific surface area of the carrier, \bar{d} is the mean diameter of pores, x_{Co} is the content of Co metal after reduction, \bar{D}_{Co} is the mean size of Co particles, σ^2 is the variance of the Co particle size distribution, S_{sp} is the specific surface area calculated from the content of the metal after reduction and the mean size of particles; the mean size and variance were determined from magnetic measurements.

we study the kinetics of oxidation of Co nanoparticles at room temperature in inert carriers with various chemical natures and porous structures often used in heterogeneous catalysis.

EXPERIMENTAL

The objects of study were prepared by the traditional method of the impregnation of carriers by a solution of Co nitrate with the required concentration. Carriers were Q-3, Q-6, Q-10, Q-15, and Q-30 CARIACT silica gels (Fujisilysia chemical ltd.) with narrow pore size distributions and alumina (Engelhard) with pore diameters 8, 10, and 20 nm. The pore size distributions and specific surface areas of silica gels were determined by low-temperature nitrogen adsorption on an ASAB 2010 adsorbtometer. Before calcining, catalysts were dried at 90°C for 10 h. Calcining was performed in a flow of air at 400°C. The volume flow rate of air was 480 h⁻¹. The 0.2% Pt/5% Co/Q-6 sample was prepared from a calcined 5% Co/Q-6 sample by impregnating it with a solution of [Pt(NH₃)₄]Cl₂.

Electron microscopic studies were performed on a JEOL 2010 transmission electron microscope at a

200 kV accelerating voltage. A sample in the form of a suspension in ethanol was deposited on a carbon film situated on a copper micronet. Electron microscopic images for the determination of Co particle-size distribution functions were processed using a program specially designed for this purpose.

A Method for Studying the Kinetics of Oxidation

Immediately before measurements, samples were reduced in a flow of hydrogen. The reactor was a measuring cell of a vibrating-coil magnetometer, which was a flow microreactor with volume 0.5 ml. The weight of samples was 26×10^{-3} g. Magnetization was assumed to be proportional to the cobalt metal weight. Reduction was performed under the conditions of linear heating at a rate of 9 K/min to $T = 973$ K at a hydrogen flow rate of 60 cm³/min. The completeness of reduction was controlled by measuring magnetization. After a constant magnetization was reached, samples were cooled to 283 K in a flow of special-purity argon.

Oxidation was performed in an O₂ + N₂ mixture at atmospheric pressure and 283 K. Saturation magnetization σ_s was determined by extrapolation to an infinite field in the $1/H - \sigma_s$ coordinates. A maximum field strength was 6.3 kOe. Magnetic field strength was determined using an RSh1-10 magnetic induction meter.

The Determination of the Size of Co Particles

Co particle-size distribution was determined using the method described in [9]. To check the applicability of this method, we studied several samples by transmission electron microscopy. The selection of samples for transmission microscopy studies was determined by the degree of “transparency” of substrates to electron beams. Samples with a low content of Co deposited on silica gel were most suitable. The table contains the mean particle sizes and distribution variances determined this way for catalysts reduced at 600°C.

RESULTS AND DISCUSSION

The Influence of CO Preadsorption and the Presence of H₂O Vapor on the Rate of Oxidation

At room temperature, a comparatively well ordered oxide film with a crystal structure close to the CoO cubic (FCC) phase [10] is formed on the surface of Co. CoO is an antiferromagnet, and a decrease in magnetization is therefore observed during oxidation. Two time stages with different cobalt oxidation rates are observed. The first fast stage ends at approximately the tenth second, and the process is then sharply decelerated. Such a dynamics is quite correctly qualitatively described by the C–M theory [2]. The first fast

stage is characterized by the formation of a thin oxide layer under the action of the Mott potential.

It was suggested in [11] that the initial rate of oxidation was proportional to the degree of metal surface coverage by atomic oxygen; that is, dissociative adsorption of oxygen occurred on the surface. To substantiate this hypothesis, we performed an experiment in which carbon monoxide was adsorbed on the surface of Co immediately before oxidation. The adsorption of CO was performed under pulsed conditions in a flow of Ar, and the amount of adsorbed CO was recorded using an IR detector situated at the exit of the reactor. During subsequent oxidation with a 23% $O_2 + N_2$ mixture, CO desorption was observed at the initial time moment probably because of the displacement of CO by adsorbed oxygen. The formation of CO_2 was not observed, but the amount of desorbed CO was smaller than that of CO initially adsorbed. It was mentioned in [12] that, during the adsorption of CO on Co at room temperature, partial disproportionation of CO with the subsequent formation of surface Co carbide was possible. Nevertheless, as mentioned, we did not observe the formation of noticeable amounts of CO_2 . Experiments showed that the preadsorption of CO noticeably decreased the rate of subsequent Co oxidation no matter what the nature of the carrier. It follows that the result obtained substantiates the earlier suggestion that the limiting process of the initial oxidation stage is the adsorption of oxygen.

The presence of Pt in samples has the opposite influence on the oxidation of cobalt nanoparticles. We then observe a substantial increase in the rate of oxidation. We believe that this is caused by the ability of platinum to dissociatively adsorb oxygen with subsequent spillover of atomic oxygen to cobalt oxide. Characteristically, an increase in the rate of oxidation is observed at both the first rapid and subsequent slow stage of the reaction.

The presence of water vapor in the oxidizing gas mixture strongly accelerates oxidation. One of the possible explanations of the acceleration of oxidation of cobalt nanoparticles by oxygen in the presence of water vapor is the predominant adsorption of H_2O , which has a lone electron pair and is a donor of electrons, on Co^{2+} ions (which are Lewis acid centers), as distinct from O_2 molecules. Electron density transfer from water molecules to metal cations occurs. An increase in electron density on the surface of oxide accelerates the diffusion of metal cations from the metallic nucleus outward, which accelerates oxidation [13].

Passivation Effects

The processes that occur in passivation of metal deposited catalysts are of interest for practical applications. We therefore made an attempt to study the kinetics of oxidation of Co nanoparticles in air directly

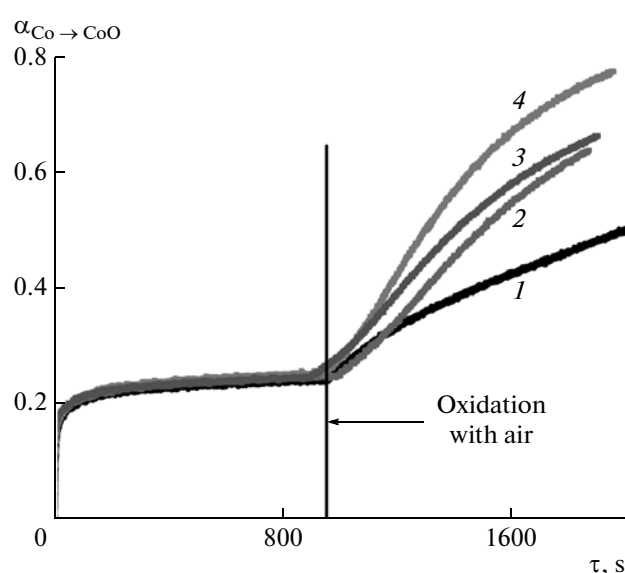


Fig. 1. Dependences of the degree of transformation on the concentration of oxygen at the passivation stage and during subsequent oxidation in a flow of air: (1) 0.2% $O_2 + N_2$, (2) 2.5% $O_2 + N_2$, (3) 5% $O_2 + N_2$, and (4) 10% $O_2 + N_2$. Vertical lines mark the moments of the replacement of oxygen mixtures with a flow of air.

after preliminary passivation in gas mixtures with various oxygen concentrations. It was found that the rate of oxidation in air noticeably depended on the concentration of oxygen during passivation.

The results of the passivation of a 5% Co/Q-6 catalyst are shown in Fig. 1. During the first 15 min, the catalyst was exposed to a flow of mixtures of oxygen with nitrogen, and mixtures were then replaced by a flow of air. This time moment is marked by a vertical line in the figure. Characteristically, at the stage of passivation, the degree of transformation is independent of oxygen concentration, as is typical Knudsen diffusion controlled processes. The rate of oxidation in an air flow increases in parallel with an increase in the concentration of O_2 at the passivation stage.

We also observe an increase in the rate of oxidation as the duration of passivation grows.

According to Fig. 1, in the oxidation of a 5% Co/Q-6 sample with a low content of cobalt, there is no dependence of the degree of $Co \rightarrow CoO$ transformation on the partial pressure of oxygen. Nevertheless, when moist air is subsequently introduced, the rate of oxidation is the higher the higher the concentration of oxygen in a passivating mixture. We believe that the higher the concentration of oxygen in a passivating mixture, the more imperfect is the oxide layer formed. It contains more cationic vacancies and voids at the metal–oxide boundary, which, accordingly, increases the rate of oxidation when air is subsequently introduced.

The duration of oxidative treatment has a similar effect. As exposure to passivating mixtures increases, the rate of subsequent oxidation in a flow of moist air grows.

Note that a substantial increase in the degree of transformation after the introduction of air is caused by the accelerating action of water vapor. The lower the partial pressure of oxygen and the shorter the time of passivation, the less imperfect oxide layer is formed under mild oxidation conditions and the more effective is passivation. It is likely that, in the limit, the passivating oxide layer must have a minimum number of defects and must be formed at the earliest stages of oxidation, when the oxide film is formed only because of the Mott potential.

The Influence of Diffusion in Carrier Pores on the Kinetics of Oxidation of Co Particles

The objects studied have developed pore structures, and it was reasonable to study the influence of diffusion on the oxidation of Co nanoparticles situated in carrier pores. A fairly large number of papers were concerned with the influence of the porous structure of carriers on the kinetics of heterogeneous including catalytic reactions under stationary conditions. The formalism developed earlier is, however, almost inapplicable to the oxidation of Co particles in porous media, because the oxidation of Co nanoparticles occurs under nonstationary conditions. The rate of oxidation of Co particles depends not only on the partial pressure of oxygen (is limited by diffusion at the initial oxidation stage) but also on the mechanism of oxidation of nanoparticles. As the reaction proceeds, the mechanism of oxidation changes. After the formation of a thin oxide film (the Cabrerra–Mott mechanism, in which the rate is limited by electric field strength between a metallic nucleus and a negatively charged external oxide surface), a fairly sharp transition to the diffusion mechanism occurs (the rate is limited by thermally activated diffusion of cobalt cations through the oxide layer). It follows that two diffusion processes with various physical natures occur simultaneously in the reaction system, diffusion of oxygen in carrier pores and diffusion of cobalt ions in the solid cobalt oxide phase. A consideration of the kinetics of oxidation of Co nanoparticles in porous media requires taking into account factors specified above.

To obtain an objective picture of the process, we must take into account the presence of a gradient of oxygen concentration in the volume of a porous carrier granule, as a result of which Co particles near the surface of the granule and in its center have different degrees of transformation into oxide at each time moment. With taking into account the passivation effect, this results in passivation of Co particles situated close to the center of the granule because of a

lower oxygen concentration. As a result, the oxidation of these particles occurs at a lower rate.

The oxidation of metals is accompanied by an exothermic effect and, in reality, the oxidation of Co nanoparticles is not an isothermal process. This in turn results in a dependence of the degree of transformation on the concentration of Co particles in a granule. At low concentrations, heat released in the oxidation of one Co particle does not influence the oxidation of neighboring Co particles because of a low heat conductivity of the porous medium. We then do not observe noticeable heating of the system as a whole.

The dependence of the degree of transformation of Co into CoO for a series of Co/Al₂O₃ samples with various mean diameters of carrier pores and low Co contents (5 wt %) is shown in Fig. 2. The observed increase in the rate of oxidation as the diameter of pores grows is evidence of the inside diffusion mechanism of the process. In addition, taking into account the size of pores and the free path of O₂ molecules at room temperature, the conclusion can be drawn that we observe Knudsen diffusion. Therefore, the diffusion coefficient is independent of the partial pressure of oxygen. Indeed, we found that the rate of oxidation was independent of the concentration of oxygen to within measurement errors at oxygen concentration less than 10% for samples with equal Co concentrations and equal diameters of pores.

To study the degree to which the oxidation of Co nanoparticles was nonisothermal, we performed experiments in which both the concentration of oxygen and the concentration of Co in porous matrices were varied. In catalyst samples with a low content of Co, we did not observe a dependence of the degree of transformation on the partial pressure of oxygen. Conversely, for samples with a high content of Co, the dependence of the degree of transformation on the concentration of O₂ was strong. Since the thickness of the oxide layer (the degree of Co transformation into CoO in our experiments) depended on temperature, an increase in the degree of transformation as the concentration of oxygen grew could be explained by exothermic effects. When the sample was diluted with an inert carrier, the effect decreased, which substantiated the hypothesis of the influence of exothermicity on the degree of transformation.

The time dependence of the degree of transformation of Co into oxide is shown in Fig. 3 for a 20% Co/Q-30 catalyst for two oxygen concentrations (0.2 and 10%). The catalyst was diluted with an inert carrier in Fig. 3a and was used in the pure form in Fig. 3b.

To more completely understand the oxidation of Co nanoparticles, it is reasonable to use a mathematical model, which clarifies the roles played by various factors and their significance in the mechanism of the reaction.

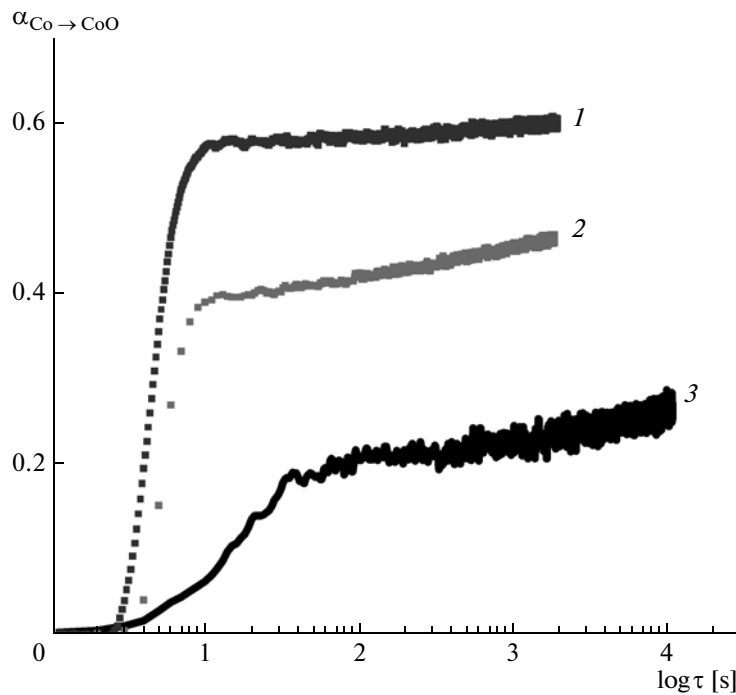


Fig. 2. Dependences of the degree of transformation of Co into CoO for a series of Co/Al₂O₃ samples with various diameters of pores during oxidation with 1% O₂ + N₂: (1) 5% Co/E90 (mean diameter of pores is $d_{av} = 20$ nm), (2) 5% Co/E200 ($d_{av} = 10$ nm), and (3) 5% Co/E380 ($d_{av} = 8$ nm).

A Mathematical Model of the Oxidation of Metal Nanoparticles in a Porous Carrier

A model of the oxidation of a nanoparticle. It is known that the oxidation of metals includes electrochemical processes, which are currently difficult to model in detail because of the complexity of processes and deficiency of information about model parameter values. For this reason, we suggest a simple phenomenological model capable of describing the observed kinetics of oxidation at a qualitative level.

In our model of oxidation of a metallic nanoparticle, we consider an abstract reaction consisting of two stages: dissociative adsorption of O₂ molecules from the gas phase onto the surface of the particle, O₂(g) + 2* = 2O, where the asterisk means an adsorption center on the surface of the particle, and the oxidation of the metal in the form M + O = MO. We can then write equations for the evolution of the mean concentration θ of oxygen atoms on the surface of the particle and the degree of particle oxidation α,

$$\begin{aligned}\dot{\theta} &= k_a c_0 (1 - \theta)^2 - k_x (1 - \alpha) \theta, \\ \dot{\alpha} &= k_v k_x (1 - \alpha) \theta,\end{aligned}\quad (1)$$

where c_0 is the volume concentration of oxygen in the gas phase.

In the right-hand side of the first equation, the $k_a = k_a c_0 (1 - \theta)^2$ term is the rate of an increase in the surface concentration of oxygen because of dissociative adsorption. It is as a rule assumed that this rate is pro-

portional to the concentration c_0 of oxygen in the gas phase and the square of the concentration of free adsorption centers on the surface of the particle, k_a is the rate constant for the adsorption of O₂. It is assumed that the number of adsorption centers (adsorption layer capacity) and the k_a constant are independent of the degree of oxidation α. The $K_x = k_x (1 - \alpha) \theta$ term is the rate of a decrease in the concentration of oxygen during metal oxidation. The rate of an increase in the degree of oxidation is $k_v K_x$, where the k_v coefficient is the ratio between the number of adsorption centers and the number of metal atoms in the particle. This ratio can be estimated using the equation

$$k_v = (r_p^3 - (r_p - l_c)^3) / r_p^3, \quad (2)$$

which is the ratio between the volume of the surface layer of atoms and the volume of the particle. Here, r_p is the radius of the particle and l_c is the metal lattice constant.

The experimental data were analyzed to select the $k_x = k_x(\alpha, r_p)$ parameter in the form of the Arrhenius exponential function with additional parameters taking into account the special features of the kinetics of the reaction,

$$k_x(\alpha, r_p) = k_x^0 \exp \left[-\frac{E_x/k_v}{RT(1 - \alpha)} \right], \quad (3)$$

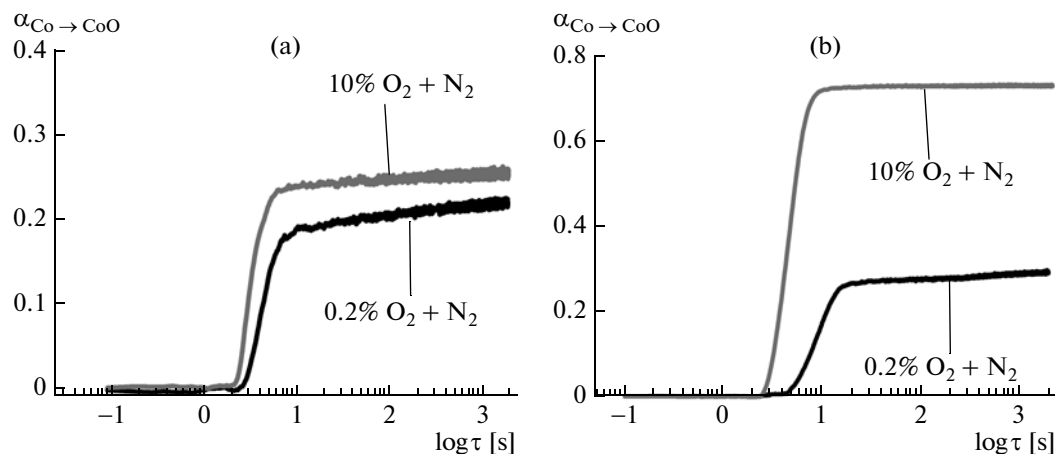


Fig. 3. Dependences of the degree of transformation on time for a 20% Co/Q-30 catalyst at two oxygen concentrations (0.2 and 10%); (a) catalyst diluted by an inert carrier and (b) pure catalyst.

where E_x is the “effective” activation energy of oxidation, R is the universal gas constant, and T is the temperature. It is known that, at least at the initial process stage, the rate of oxidation increases as the size of the particle decreases. In addition, at the slow state, the degree of oxidation of small particles is higher compared with large particles. The k_v parameter takes into account the influence of the size of particles on the rate of oxidation at the initial (fast) reaction stage. At the slow stage, the rate of oxidation tends to zero as $\alpha \rightarrow 1$. This is taken into account in (3) by the $(1 - \alpha)^{-1}$ multiplier in the exponent.

The time dependences of the degree of oxidation of particles with various diameters (m) are shown in Fig. 4. The dependences were obtained using the parameters $T = 300$ K; $c_0 = 1.71 \times 10^{-4}$ g/cm³, which corresponds to a 10 torr partial pressure of oxygen; $k_a = 2.06 \times 10^5$ cm³/(g s), $k_x^0 = 10^{15}$ s⁻¹, $E_x = 10$ kJ/mol. The influence of the size of particles on the

degree of oxidation qualitatively corresponds to the experimental data.

A Model of the Oxidation of Nanoparticles in a Porous Granule

Metal nanoparticles are situated in inert carrier pores in metal deposited catalysts. It follows that a catalyst consists of porous grains or granules containing nanoparticles. For simplicity, let a granule be a sphere with radius R_g . Its volume and mass are then $V_g = (4/3)\pi R_g^3$ and $M_g = \rho_g V_g$, respectively, where ρ_g is the specific gravity of the material of granules. The mass of a metal in a granule is determined through its percent content in the catalyst, p_m , by the equation $M_m = (p_m M_g)/(100 - p_m)$. Suppose that metal particles are equally sized balls with radius r_p . The volume of such a ball is $V_p = (4/3)\pi r_p^3$, and its mass is $\rho_p V_p$. It follows that, if all particles are equally sized, the granule contains $N_p = M_m/(\rho_p V_p)$ metal particles. We assume for simplicity that metal particles are uniformly distributed over the volume of the granule. The number of particles in a spherical granule layer r , $r + dr$ is then calculated by the equation $dN_p(r) = (N_p/V_g)4\pi r^2 dr$.

During time dt , $dN_{\text{O}_2}(r, t) = (1/2)N_a dN_p K_a(r, t) dt$ oxygen molecules are adsorbed on the surface of nanoparticles in the $(r, r + dr)$ granule spherical layer. The volume concentration of oxygen in pores in a spherical layer therefore changes by $dc(r, t) = m_{\text{O}_2} dN_{\text{O}_2}(r, t)/dV_\gamma(r)$, where N_a is the number of adsorption centers on the surface of a nanoparticle, m_{O_2} is the mass of the oxygen molecule, $dV_\gamma(r) = 4\pi r^2 dr$ is the volume of pores in a spherical layer, and γ is the porosity coefficient. N_a can be estimated using

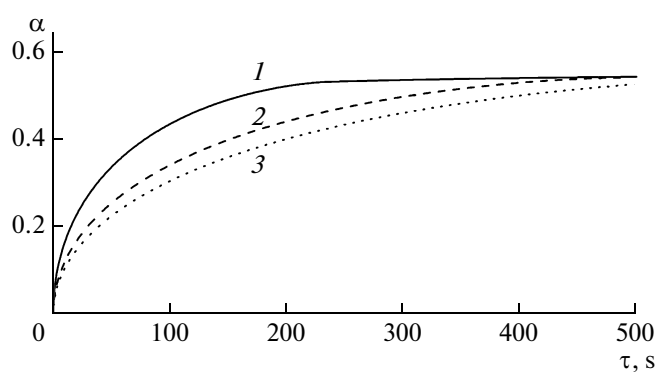


Fig. 4. Influence of diffusion on the kinetics of oxidation of Co: (1) $D_1 = 10^{-2}$ cm²/s, (2) $D_2 = D_1/2$, and (3) $D_3 = D_2/4$.

the equation $N_a \approx 4\pi r_p^2 / \pi l^2$, where l is the metal lattice constant. We eventually obtain that the rate of changes in the concentration of oxygen in granule pores caused by adsorption onto the surface of nanoparticles is $(a/2\gamma)K_a$, where $a = m_{O_2} N_a V_p / V_g$.

On the assumption that the diffusion flux of oxygen in granule pores is proportional to the gradient of concentration (the Fick law), we obtain a system of equations for the concentration of oxygen in pores $c(r, t)$, surface concentration of oxygen $\theta(r, t)$, and the degree of oxidation $\alpha(r, t)$,

$$\begin{aligned}\frac{\partial c}{\partial t} &= \frac{1}{r^2} \frac{\partial}{\partial r} \left(\gamma D r^2 \frac{\partial c}{\partial r} \right) - \frac{a}{2\gamma} k_a c (1 - \theta)^2, \\ \frac{\partial x}{\partial t} &= k_a c (1 - \theta)^2 - k_x (1 - \alpha) \theta, \\ \frac{\partial \alpha}{\partial t} &= k_v k_x (1 - \alpha) \theta.\end{aligned}\quad (4)$$

Calculations are performed with augmenting Eqs. (4)

by the boundary conditions $\frac{\partial c}{\partial r} \Big|_{r=R_g} = h_c (c_0 - c)$ and $\lim_{r \rightarrow 0} \left(r \frac{\partial c}{\partial r} \right) = 0$ and zero initial conditions.

Equations (4) were solved numerically with the parameters $R_g = 1$ mm, $\rho_g = 3.3$ g/cm³, $p_m = 10\%$, $r_p = 3$ nm, and $l = 0.25$ nm. Oxidation model parameter values are the same as in Fig. 4.

It follows from calculations that the rate of oxidation decreases as the rate of oxygen diffusion in granule pores lowers. This result is in qualitative agreement with the experimental data on the oxidation in carriers with different pore sizes. Note that, as distinct from the experimental data, the degrees of oxidation in various carriers calculated by (4) tend to one value with time. This likely means that model (4) ignores certain important factors (for instance, cobalt passivation, temperature changes, etc.). Also note that we assumed in calculations that $\gamma = 1$ because of the absence of data on the porosity of carriers.

The experimental kinetics of oxidation depends on oxygen pressure (see Fig. 3b). This dependence can be explained by the influence of temperature on the rate of oxidation. To check this possibility, we constructed the following nonisothermal model of oxidation (5), in which the heat conductivity equation at temperature T was added to the model (4) equations,

$$\begin{aligned}\frac{\partial c}{\partial t} &= \frac{1}{r^2} \frac{\partial}{\partial r} \left(\gamma D r^2 \frac{\partial c}{\partial r} \right) - F(c, x), \\ \frac{\partial T}{\partial t} &= \frac{1}{r^2} \frac{\partial}{\partial r} \left(\lambda r^2 \frac{\partial T}{\partial r} \right) + Q(x, y), \\ \frac{\partial x}{\partial t} &= k_a c (1 - x)^2 - k_x (1 - \alpha) x, \\ \frac{\partial \alpha}{\partial t} &= k_v k_x (1 - \alpha) x.\end{aligned}\quad (5)$$

The rate of temperature changes in the oxidation reaction is $Q = \frac{q p_m}{\rho_g c_g} \frac{\partial \alpha}{\partial t}$, where q is the heat effect of the reaction. The boundary conditions for temperature have the same form as the boundary conditions for oxygen concentration; that is, zero flux in the center of a granule and condition of the third kind at the external boundary.

Numerical modeling shows that the rate of the reaction increases as the partial pressure of oxygen grows. Note that, in model (1)–(3) of the oxidation of one particle without taking oxygen diffusion in pores into account, the rate of oxidation was almost independent of oxygen pressure. The pressure dependence of the rate is caused by diffusion deceleration and the nonisothermal character of the reaction. Taking only diffusion deceleration into account leads to a kinetics that qualitatively differs from the experimental data. The inclusion of temperature effects remedies this shortcoming of the model.

In model (5), the degrees of oxidation at the slow reaction stage (at long times) depend on pressure, and the higher the pressure of oxygen the larger the degree of oxidation at the slow reaction stage. This difference increases as the mass of a metal grows. It follows from the plot of temperature changes (Fig. 5) that a substantial increase in the mean temperature of a granule is observed at the fast reaction stage, which determines the degree of oxidation at the slow stage. The higher the pressure of oxygen the higher the temperature at the fast stage and, accordingly, the higher the degree of oxidation. The amount of heat released during the reaction increases as the mass of a metal grows. For this reason, for the sample with $p_m = 20\%$, the temperature at the fast stage is much higher than for the sample with $p_m = 5\%$. Therefore, the difference between the degrees of oxidation at the slow stage is larger.

To summarize, we showed that the limiting stage of the reaction was the dissociative adsorption of oxygen molecules resulting in the oxidation of surface cobalt atoms. After the formation of a continuous cobalt oxide layer on the surface of particles, the Mott potential value becomes the rate limiting factor. This value is independent of the partial pressure of oxygen in the oxidation of Co particles. The Mott potential increases the mobility of cobalt cations through the oxide layer and contributes to tunneling of electrons from the metallic nucleus to oxygen molecules adsorbed on the outside oxide surface.

The partial pressure of oxygen substantially influences the imperfection of the oxide layer in low-temperature oxidation. On the other hand, this results in a dependence of the effective passivation of Co nanoparticles on the time of passivation and the partial pressure of oxygen. On the other hand, this causes the passivation of cobalt particles in “narrow” carrier pores and a dependence of the rate of oxidation and

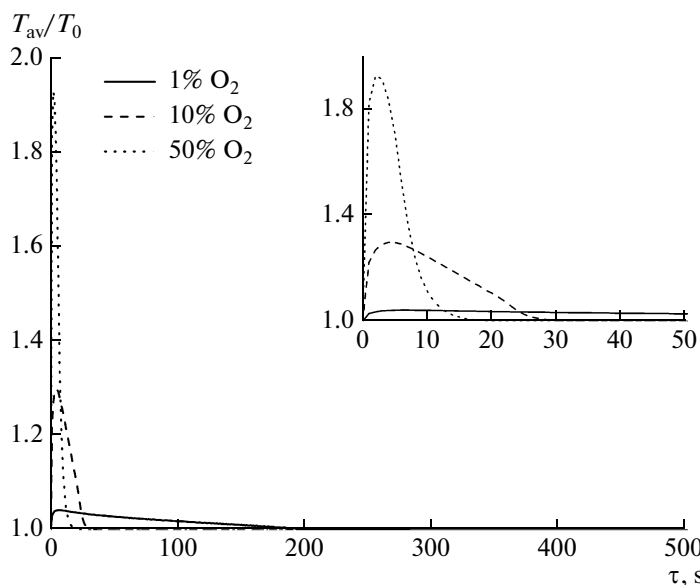


Fig. 5. Relative changes in the mean temperature of a granule, T_{av}/T_0 .

the degree of $\text{Co} \rightarrow \text{CoO}$ transformation on the diameter of carrier pores.

After the end of the fast stage, process develops in the diffusion mode, the rate of oxidation of metal nanoparticles is limited by the diffusion of metal ions and oxygen through the oxide layer. For cobalt, $D_{\text{Co}} \gg D_{\text{O}_2}$, and the rate determining stage is therefore the diffusion of cobalt cations through the oxide layer. The diffusion coefficient of cobalt cations in the reaction under elevated temperature conditions increases as the partial pressure of oxygen at the oxide/gas boundary grows. The rate of oxidation and the final degree of $\text{Co} \rightarrow \text{CoO}$ transformation therefore increase as the partial pressure of oxygen grows.

For samples with high cobalt contents (11–20 wt %), local heat release begins to substantially influence the reaction. The reaction passes from the kinetic oxidation mode to the diffusion mode characterized by a dependence of the degree of transformation on the partial pressure of oxygen and the absence of such a dependence on the size of cobalt crystallites. An increase in the concentration of cobalt increases the amount of heat released in the reaction and local temperature and, in the absence of diffusion limitations and at high oxygen partial pressures, results in an increase in the rate of the reaction and the final degree of $\text{Co} \rightarrow \text{CoO}$ transformation.

The suggested mathematical model quite correctly describes the processes that occur in the system and

gives a qualitatively correct explanation of experimental observations.

REFERENCES

1. C. Wagner, Z. Phys. Chem. Abt. B **21**, 25 (1933).
2. N. F. Caberra and N. Mott, Rep. Prog. Phys. **12**, 163 (1948–1949).
3. V. P. Zhdanov and Bengt Kasemo, Chem. Phys. Lett. **452**, 285 (2008).
4. A. D. Smigelskas and E. O. Kirkendall, Trans. AIME **171**, 130 (1947).
5. Y. Yin, R. M. Riou, C. K. Erdonmez, et al., Science **304**, 711 (2004).
6. C. M. Wang, D. R. Baer, L. E. Thomas, et al., J. Appl. Phys. **98**, 094308 (2005).
7. P. A. Chernavskii, G. V. Pankina, V. I. Zaikovskii, et al., J. Phys. Chem. C **112**, 9573 (2008).
8. H. J. Fan, M. Knez, R. Scholz, et al., Nano Lett. **7**, 993 (2007).
9. P. A. Chernavskii, Vei Chu, A. Yu. Khodakov, et al., Zh. Fiz. Khim. **82**, 83 (2008) [Russ. J. Phys. Chem. A **82**, 951 (2008)].
10. S. W. Charles and S. Linderoth, J. Magn. Magn. Mater. **196–197**, 18 (1999).
11. P. A. Chernavskii, G. V. Pankina, A. P. Chernavskii, et al., J. Phys. Chem. C **111**, 5576 (2007).
12. Rao K. Mohana, D. Scarano, G. Spoto, and A. Zecchina, Surf. Sci. **204**, 319 (1988).
13. S. R. J. Saunders, M. Monteiro, and F. Rizzo, Progress Mater. Sci. **53**, 775 (2008).